



TIME-FREQUENCY-AUTOREGRESSIVE RANDOM PROCESSES: MODELING AND FAST PARAMETER ESTIMATION

Michael Jachan, Gerald Matz, and Franz Hlawatsch

Institute of Communications and Radio-Frequency Engineering, Vienna University of Technology
Gusschausstrasse 25/389, A-1040 Wien, Austria (Europe)
phone: +43 1 58801 38914, fax: +43 1 58801 38999, email: michael.jachan@tuwien.ac.at
web: www.nt.tuwien.ac.at/dspgroup/time.html

ABSTRACT

We present a novel formulation of nonstationary autoregressive (AR) models in terms of time-frequency (TF) shifts. The parameters of the proposed *TFAR model* are determined by “TF Yule-Walker equations” that involve the expected ambiguity function and can be solved efficiently due to their block-Toeplitz structure. For moderate model orders, we also propose approximate TF Yule-Walker equations that have Toeplitz/block-Toeplitz structure and thus allow a further reduction of computational complexity. Simulation results demonstrate that the TFAR model is parsimonious and accurate and that the performance of our parameter estimation methods compares favorably with that of Grenier’s method.

1. INTRODUCTION

A stationary autoregressive (AR) process $x[n]$ is defined by [1, 2]

$$x[n] = -\sum_{m=1}^M a_m x[n-m] + e[n] = -\sum_{m=1}^M a_m (\mathbb{S}^m x)[n] + e[n], \quad (1)$$

where \mathbb{S} denotes the time shift operator acting as $(\mathbb{S}x)[n] = x[n-1]$, the a_m are the AR model parameters, M is the AR model order, and $e[n]$ is stationary white innovations noise. Because many real-world processes are nonstationary, *nonstationary AR* models of the form

$$x[n] = -\sum_{m=1}^M a_m[n] x[n-m] + e[n] \quad (2)$$

have been introduced in [3, 4], along with basis expansion techniques for modeling and estimating the parameters $a_m[n]$. Nonstationary AR (and ARMA) parameter estimation using basis expansions was further developed by Grenier [5] and others [6–9].

In this paper, we present a different viewpoint of nonstationary AR models that is based on time-frequency (TF) shifts. The proposed *TFAR model* is described in Section 2. In Section 3, we derive “TF Yule-Walker equations” for estimation of the model parameters. A relation of TFAR modeling with nonstationary linear prediction is discussed in Section 4. Section 5 presents fast algorithms for the solution of the TF Yule-Walker equations. Finally, simulation results provided in Section 6 demonstrate the good performance of the TFAR model and our parameter estimation methods.

2. THE TFAR MODEL

In the following, all signals will be defined on the interval $[0, N-1]$. A basic difference between time-invariant and time-varying linear systems is that the latter introduce frequency shifts in addition to time shifts. Motivated by this observation, we propose the following nonstationary extension of the stationary AR model (1):

$$x[n] = -\sum_{m=1}^M \sum_{l=-L}^L a_{m,l} (\mathbb{M}^l \mathbb{S}^m x)[n] + e[n] \quad (3a)$$

$$= -\sum_{m=1}^M \sum_{l=-L}^L a_{m,l} e^{j \frac{2\pi}{N} ln} x[n-m] + e[n]. \quad (3b)$$

Funding by FWF grant P15156.

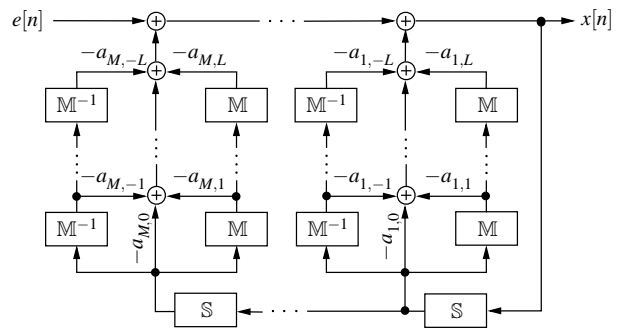


Figure 1: Block diagram of the TFAR model of order (M, L) .

Here, \mathbb{M} is the frequency shift (modulation) operator that is defined by $(\mathbb{M}x)[n] = e^{j \frac{2\pi}{N} ln} x[n]$, the $a_{m,l}$ are model parameters, M is the temporal (delay) model order, and L is the spectral (Doppler) model order. Furthermore, the innovations noise $e[n]$ now is *nonstationary* white with time-dependent variance $\sigma^2[n]$. We will call (3) a *TFAR model of order (M, L)* . The generation of $x[n]$ is illustrated in Fig. 1.

Evidently, (3b) is equivalent to (2) with

$$a_m[n] = \sum_{l=-L}^L a_{m,l} e^{j \frac{2\pi}{N} ln}. \quad (4)$$

Thus, the parameter functions $a_m[n]$ are bandlimited with (normalized) bandwidth L/N . For slowly time-varying $a_m[n]$, a small spectral model order L suffices, and thus the number of parameters in (3), $(2L+1)M$, is much less than that in (2), NM . We note that (4) is a special case of the basis expansion technique used in [3–5]. The advantage of our novel formulation in terms of frequency shifts is that it adds physical intuition and leads to new, improved TF techniques for parameter estimation (see Section 3).

For modeling the time-varying driving noise variance $\sigma^2[n]$, we use a bandlimited Fourier basis expansion similar to (4):

$$\sigma^2[n] = \sum_{l=-2L}^{2L} \sigma_l e^{j \frac{2\pi}{N} ln}. \quad (5)$$

(We use bandwidth $2L$ because $\sigma^2[n]$ is a “squared” quantity.) Thus, the parameters of the TFAR model are given by the $(2L+1)M$ coefficients $a_{m,l}$ and the $2L+1$ coefficients σ_l (note that $\sigma_{-l} = \sigma_l^*$).

3. TF YULE-WALKER EQUATIONS

In this section, we derive Yule-Walker type equations that allow to calculate (estimate) the TFAR parameters $a_{m,l}$.

Yule-Walker Type Equations. The conventional Yule-Walker equations [1, 2] relate the parameters a_m of a stationary AR process to the autocorrelation function of the process. Similar equations can

be derived for a TFAR process by multiplying (3b) by $x^*[n-m]$ and taking expectation. This yields

$$r_x[n, m] = - \sum_{m'=1}^M \sum_{l'=-L}^L a_{m', l'} e^{j \frac{2\pi}{N} l' n} r_x[n-m', m-m'] + r_{e, x}[n, m], \quad (6)$$

with the autocorrelation function $r_x[n, m] \triangleq \mathbb{E}\{x[n]x^*[n-m]\}$ and the crosscorrelation function $r_{e, x}[n, m] \triangleq \mathbb{E}\{e[n]x^*[n-m]\}$. It can be shown that $r_{e, x}[n, m] = h^*[n-m, -m]$, where $h[n, m]$ denotes the impulse response of the TFAR system \mathbb{H} that maps $e[n]$ to $x[n] = (\mathbb{H}e)[n]$. Because \mathbb{H} is causal, $h[n, m] = 0$ for $m < 0$ and thus $r_{e, x}[n, m] = h^*[n-m, -m] = 0$ for $m > 0$. Hence, we obtain

$$r_x[n, m] = - \sum_{m'=1}^M \sum_{l'=-L}^L a_{m', l'} e^{j \frac{2\pi}{N} l' n} r_x[n-m', m-m'], \quad m > 0. \quad (7)$$

The parameters $a_{m, l}$ could be calculated from these equations. However, we have $(N-1)M$ equations for the $(2L+1)M$ parameters, i.e., certain equations are linearly dependent and a subset of $(2L+1)M$ linearly independent equations is not easily determined. In practice, this was observed to result in poor parameter estimates when the autocorrelation function $r_x[n, m]$ is replaced by an estimate.

TF Yule-Walker Equations. We now propose a method that avoids this problem. Taking the length- N discrete Fourier transform ($n \rightarrow l$) of both sides of (7) yields

$$\bar{A}_x[m, l] = - \sum_{m'=1}^M \sum_{l'=-L}^L a_{m', l'} \bar{A}_x[m-m', l-l'] e^{-j \frac{2\pi}{N} m' (l-l')}, \quad m > 0, \quad (8)$$

where

$$\bar{A}_x[m, l] \triangleq \sum_{n=0}^{N-1} r_x[n, m] e^{-j \frac{2\pi}{N} ln} \quad (9)$$

is the *expected ambiguity function* (EAF) of $x[n]$ (cf. [10, 11]). The EAF has a physically meaningful interpretation as a TF correlation function of $x[n]$, i.e., it characterizes statistical correlations between process components that are separated in time by m and in frequency by l . Estimation of the EAF will be discussed presently.

It can be shown that for $m \in [1, M]$ and $l \in [-L, L]$, (8) indeed yields a system of $(2L+1)M$ linearly independent equations in the $(2L+1)M$ parameters $a_{m, l}$. This system of equations will be termed *TF Yule-Walker equations*. (Related equations were obtained in [5] via a different approach, without noticing the connection to the EAF. Simulation results provided in Section 6 indicate that the performance of our method is superior to that in [5].) An efficient algorithm for solving the TF Yule-Walker equations will be considered in Section 5.

Approximate TF Yule-Walker Equations. Within the relevant index range $m \in [1, M]$ and $l \in [-L, L]$, the deviation of the phase factor $e^{-j \frac{2\pi}{N} m' (l-l')}$ in (8) from 1 is bounded as

$$\max_{\substack{m' \in [1, M] \\ l, l' \in [-L, L]}} |1 - e^{-j \frac{2\pi}{N} m' (l-l')}| = 2 \left| \sin \left(\frac{\pi M L}{N} \right) \right| \leq 2\pi \frac{ML}{N}.$$

Therefore, if $ML \ll N$, we have $e^{-j \frac{2\pi}{N} m' (l-l')} \approx 1$ and thus (8) can be approximated for $m \in [1, M]$, $l \in [-L, L]$ as

$$\bar{A}_x[m, l] \approx - \sum_{m'=1}^M \sum_{l'=-L}^L a_{m', l'} \bar{A}_x[m-m', l-l']. \quad (10)$$

These *approximate TF Yule-Walker equations* involve a two-dimensional (2-D) convolution that is perfectly analogous to the 1-D convolution of the stationary case [1, 2]. They can be solved even more efficiently than the exact equations (see Section 5).

Calculation of Noise Variance Parameters. It remains to calculate the parameters σ_l in (5). With $r_{e, x}[n, 0] = \sigma^2[n]$, (6) implies

$$\sigma^2[n] = r_x[n, 0] + \sum_{m'=1}^M \sum_{l'=-L}^L a_{m', l'} e^{j \frac{2\pi}{N} l' n} r_x[n-m', -m']. \quad (11)$$

Inserting (5) and taking the length- N DFT of (11), we obtain

$$\sigma_l = \bar{A}_x[0, l] + \sum_{m'=1}^M \sum_{l'=-L}^L a_{m', l'} \bar{A}_x[-m', l-l'] e^{-j \frac{2\pi}{N} m' (l-l')}. \quad (12)$$

This expression allows to calculate the noise variance parameters σ_l after the TFAR coefficients $a_{m, l}$ have been obtained.

Estimation of the EAF. The equations (8), (10), and (12) involve the EAF $\bar{A}_x[m, l]$ in (9), which has to be estimated from the observed signal $x[n]$. The EAF can be expressed as $\bar{A}_x[m, l] = \mathbb{E}\{A_x[m, l]\}$, with the *ambiguity function*

$$A_x[m, l] = \sum_{n=0}^{N-1} x[n] x^*[n-m] e^{-j \frac{2\pi}{N} ln}.$$

Thus, a trivial unbiased estimator of the EAF is $\hat{A}_x[m, l] = A_x[m, l]$. However, it can be shown that the relative variance of this estimator increases with growing m and l . This problem can be alleviated (at the expense of a nonzero bias) by multiplying $A_x[m, l]$ by a 2-D weight function $\Psi[m, l]$ that is 1 at $(m, l) = (0, 0)$ and gradually decays for growing m, l . More generally, if I realizations $x_i[n]$ are available, we propose to use the EAF estimator

$$\hat{A}_x[m, l] = \Psi[m, l] \sum_{i=1}^I A_{x_i}[m, l]. \quad (13)$$

This estimator is related to previously proposed estimators of the Wigner-Ville spectrum [12] via a 2-D Fourier transform. For simplicity, we can use $\Psi[m, l] = w_1[m] w_2[l]$ where $w_1[m]$ and $w_2[l]$ should be adapted to the temporal and spectral correlation widths of $x[n]$. For example, for a quasi-stationary process $w_2[l]$ should be narrow, and for a quasi-white process $w_1[m]$ should be narrow.

We note that $\hat{A}_x[m, l]$ is required only for $(m, l) \in [1, M] \times [-L, L]$, i.e., typically close to the origin. This is advantageous because these EAF estimates have the smallest bias and variance; furthermore, significant computational savings can be obtained [13].

4. RELATION TO NONSTATIONARY PREDICTION

There exists a relation between the TFAR model and nonstationary linear prediction which extends that of the stationary case [1, 2, 14]. Consider the prediction of a nonstationary process $x[n]$ using a linear, time-varying filter with maximum delay M and maximum normalized Doppler frequency shift L/N , i.e.,

$$\hat{x}[n] = - \sum_{m=1}^M \sum_{l=-L}^L a_{m, l} (\mathbb{M}^l \mathbb{S}^m x)[n] = - \sum_{m=1}^M \sum_{l=-L}^L a_{m, l} e^{j \frac{2\pi}{N} ln} x[n-m]. \quad (14)$$

By definition, the optimum predictor coefficients $a_{m, l}$ minimize the mean energy $\bar{E}_e \triangleq \mathbb{E}\{\|e\|^2\}$ of the prediction error $e[n] \triangleq x[n] - \hat{x}[n]$. Due to the orthogonality principle [1], there must be $\mathbb{E}\{\langle e, \mathbb{M}^l \mathbb{S}^m x \rangle\} = \mathbb{E}\{\sum_{n=0}^{N-1} e[n] (\mathbb{M}^l \mathbb{S}^m x)^*[n]\} = 0$ for $m \in [1, M]$, $l \in [-L, L]$. This is a system of equations in the predictor coefficients $a_{m, l}$ that is easily shown to be identical to the TF Yule-Walker equations. Thus, the optimum predictor coefficients $a_{m, l}$ are equal to the TFAR parameters.

With (14), the prediction error $e[n] = x[n] - \hat{x}[n]$ is obtained as

$$e[n] = \sum_{m=0}^M \sum_{l=-L}^L a_{m, l} (\mathbb{M}^l \mathbb{S}^m x)[n] = \sum_{m=0}^M \sum_{l=-L}^L a_{m, l} e^{j \frac{2\pi}{N} ln} x[n-m], \quad (15)$$

with $a_{0, l} \triangleq \delta[l]$. This relation is equivalent to (3). Thus, the above time-varying, “TFMA-type” prediction error filter that maps $x[n]$ to $e[n]$ is inverse to the TFAR filter that maps $e[n]$ to $x[n]$ in (3). There-

fore, the prediction error $e[n]$ in (15) equals the innovations noise process $e[n]$ in (3). If estimated coefficients are used in (15) instead of the true coefficients $a_{m,l}$, the prediction error is an estimate of the innovations process. Hence, similarly to the stationary case [1, 2], the model order (M, L) can be estimated by choosing (M, L) such that the energy $\|e\|^2$ of the prediction error $e[n]$ in (15)—using the $a_{m,l}$ calculated from the TF Yule–Walker equations—is minimized.

5. FAST SOLUTION OF TF YULE-WALKER EQUATIONS

In the stationary case, the convolution structure of the Yule–Walker equations results in a matrix equation with Toeplitz structure, which can be solved efficiently using e.g. the Levinson algorithm [1, 2]. We now consider efficient algorithms for solving the TF Yule–Walker equations (both exact and approximate versions).

Exact TF Yule–Walker Equations. The coefficients of the TF Yule–Walker equations (8) are of the form $\bar{A}_x[m-m', l] e^{-j\frac{2\pi}{N}m'l}$ where $m, m' \in [1, M]$ and $l \in [-2L, 2L]$. For fixed l , there are M^2 such coefficients. They can be arranged in an $M \times M$ matrix given by $\tilde{\mathbf{A}}_l = \mathbf{A}_l \mathbf{V}_l$, where \mathbf{A}_l is an $M \times M$ Toeplitz matrix defined as

$$\mathbf{A}_l = \begin{bmatrix} \bar{A}_x[0, l] & \cdots & \bar{A}_x[-M+1, l] \\ \vdots & \ddots & \vdots \\ \bar{A}_x[M-1, l] & \cdots & \bar{A}_x[0, l] \end{bmatrix} \quad (16)$$

and $\mathbf{V}_l = \text{diag}\{e^{-j\frac{2\pi}{N}l}, e^{-j\frac{2\pi}{N}2l}, \dots, e^{-j\frac{2\pi}{N}Ml}\}$. We next define

$$\tilde{\mathbf{A}} = \begin{bmatrix} \tilde{\mathbf{A}}_0 & \cdots & \tilde{\mathbf{A}}_{-2L} \\ \vdots & \ddots & \vdots \\ \tilde{\mathbf{A}}_{2L} & \cdots & \tilde{\mathbf{A}}_0 \end{bmatrix}, \quad \mathbf{a} = \begin{bmatrix} \mathbf{a}_{-L} \\ \vdots \\ \mathbf{a}_L \end{bmatrix}, \quad \boldsymbol{\theta} = \begin{bmatrix} \boldsymbol{\theta}_{-L} \\ \vdots \\ \boldsymbol{\theta}_L \end{bmatrix},$$

with the length- M vectors $\mathbf{a}_l = [\bar{A}_x[1, l] \cdots \bar{A}_x[M, l]]^T$ and $\boldsymbol{\theta}_l = [a_{1,l} \cdots a_{M,l}]^T$. $\tilde{\mathbf{A}}$ is a $(2L+1)M \times (2L+1)M$ block-Toeplitz matrix and \mathbf{a} and $\boldsymbol{\theta}$ have length $(2L+1)M$. We can now rewrite (8) as

$$\tilde{\mathbf{A}}\boldsymbol{\theta} = -\mathbf{a},$$

so that $\boldsymbol{\theta} = -\tilde{\mathbf{A}}^{-1}\mathbf{a}$. The block-Toeplitz matrix $\tilde{\mathbf{A}}$ can be inverted by means of the fast algorithm described in [15], whose computational complexity is proportional to $(2L+1)^2 M^3$. Alternatively, if a different stacking (first with respect to l and then with respect to m) is used to construct $\tilde{\mathbf{A}}$, the complexity is proportional to $(2L+1)^3 M^2$.

Approximate TF Yule–Walker Equations. The approximate TF Yule–Walker equations (10) can also be written as $\mathbf{A}\boldsymbol{\theta} = -\mathbf{a}$, with \mathbf{a} and $\boldsymbol{\theta}$ as before and with the $(2L+1)M \times (2L+1)M$ matrix

$$\mathbf{A} = \begin{bmatrix} \mathbf{A}_0 & \cdots & \mathbf{A}_{-2L} \\ \vdots & \ddots & \vdots \\ \mathbf{A}_{2L} & \cdots & \mathbf{A}_0 \end{bmatrix},$$

where the \mathbf{A}_l were defined in (16). Since \mathbf{A} is a Toeplitz/block-Toeplitz matrix, this equation can be solved using the efficient algorithm described in [16] (we note that a multichannel Levinson algorithm cannot be used since $\mathbf{A}_l \neq \mathbf{A}_l^H$ in general).

We will now formulate a version of this algorithm that is order-recursive with respect to the spectral model order L , using a fixed temporal model order M . The complexity of this algorithm is again proportional to $(2L+1)^2 M^3$, but the proportionality factor is only half that of the previously mentioned algorithm for the exact TF Yule–Walker equations. (Again, using a different stacking to construct \mathbf{A} yields a fast algorithm that is order-recursive with respect to M , with a fixed L . The complexity then is proportional to $(2L+1)^3 M^2$, again with half the proportionality factor of the exact case.)

Assume that we have solved the k th-order equation $\mathbf{A}^{(k)}\boldsymbol{\theta}^{(k)} = -\mathbf{a}^{(k)}$, i.e., we know $\boldsymbol{\theta}^{(k)}$. Here, $k \in \{1, \dots, 2L+1\}$, and $\mathbf{A}^{(k)}$ and $\mathbf{a}^{(k)}$ consist of the first k blocks of \mathbf{A} and \mathbf{a} , respectively:

$$\mathbf{A}^{(k)} = \begin{bmatrix} \mathbf{A}_0 & \cdots & \mathbf{A}_{-k+1} \\ \vdots & \ddots & \vdots \\ \mathbf{A}_{k-1} & \cdots & \mathbf{A}_0 \end{bmatrix}, \quad \mathbf{a}^{(k)} = \begin{bmatrix} \mathbf{a}_{-L} \\ \vdots \\ \mathbf{a}_{-L+k-1} \end{bmatrix}.$$

(Note, however, that $\boldsymbol{\theta}^{(k)}$ is not equal to the first k blocks of $\boldsymbol{\theta}$). Exploiting the block-Toeplitz structure of \mathbf{A} , we can write the system of order $k+1$ (and dimension $(k+1)M \times (k+1)M$) as

$$\begin{bmatrix} \mathbf{A}^{(k)} & \mathbf{T}_k \\ \mathbf{S}_k^T & \mathbf{A}_0 \end{bmatrix} \boldsymbol{\theta}^{(k+1)} = -\begin{bmatrix} \mathbf{a}^{(k)} \\ \mathbf{a}_{-L+k} \end{bmatrix}, \quad (17)$$

with $\mathbf{S}_k^T = [\mathbf{A}_k \cdots \mathbf{A}_1]$ and $\mathbf{T}_k = [\mathbf{A}_{-k}^T \cdots \mathbf{A}_{-1}^T]^T$. Using the matrix inversion lemma [1], the solution of (17) can be written as an update of the solution $\boldsymbol{\theta}^{(k)}$ computed previously:

$$\boldsymbol{\theta}^{(k+1)} = \begin{bmatrix} \boldsymbol{\theta}^{(k)} \\ \mathbf{0} \end{bmatrix} - \begin{bmatrix} \mathbf{W}_k \\ \mathbf{I} \end{bmatrix} \mathbf{D}_k^{-1} (\mathbf{V}_k^T \mathbf{a}^{(k)} + \mathbf{a}_{-L+k}). \quad (18)$$

Here, the matrices \mathbf{V}_k and \mathbf{W}_k are obtained using the recursions

$$\mathbf{V}_{k+1} = \begin{bmatrix} \mathbf{0} \\ \mathbf{V}_k \end{bmatrix} - \begin{bmatrix} \mathbf{E} \\ \mathbf{E}_k \mathbf{W}_k \end{bmatrix} \mathbf{D}_k^{-1} \mathbf{C}_k, \quad (19a)$$

$$\mathbf{W}_{k+1} = \begin{bmatrix} \mathbf{0} \\ \mathbf{W}_k \end{bmatrix} - \begin{bmatrix} \mathbf{E} \\ \mathbf{E}_k \mathbf{V}_k \end{bmatrix} \mathbf{D}_k^{-T} \mathbf{B}_k, \quad (19b)$$

with the “exchange” matrices

$$\mathbf{E} = \begin{bmatrix} 0 & \cdots & 1 \\ 1 & \ddots & 0 \end{bmatrix}, \quad \mathbf{E}_k = \begin{bmatrix} \mathbf{0} & \cdots & \mathbf{E} \\ \mathbf{E} & \ddots & \mathbf{0} \end{bmatrix}$$

of size $M \times M$ and $kM \times kM$, respectively. Furthermore, (18) and (19) involve $M \times M$ matrices \mathbf{D}_k , \mathbf{C}_k , and \mathbf{B}_k that are given by

$$\begin{aligned} \mathbf{D}_{k+1} &= \mathbf{D}_k - \mathbf{C}_k^T \mathbf{D}_k^{-T} \mathbf{B}_k, \\ \mathbf{C}_{k+1} &= \mathbf{V}_k^T \mathbf{E}_k \mathbf{S}_k + \mathbf{E} \mathbf{A}_{k+1}^T, \\ \mathbf{B}_{k+1} &= \mathbf{W}_k^T \mathbf{E}_k \mathbf{T}_k + \mathbf{E} \mathbf{A}_{-k-1}. \end{aligned}$$

This recursion is initialized by $\mathbf{D}_0 = \mathbf{A}_0$, $\mathbf{C}_0 = \mathbf{E} \mathbf{A}_1^T$, $\mathbf{B}_0 = \mathbf{E} \mathbf{A}_{-1}$, $\mathbf{V}_0 = -\mathbf{E} \mathbf{D}_0^{-1} \mathbf{C}_0$, and $\mathbf{W}_0 = -\mathbf{E} \mathbf{D}_0^{-T} \mathbf{B}_0$. The recursion stops at $k = 2L+1$, and the solution of $\mathbf{A}\boldsymbol{\theta} = -\mathbf{a}$ is then obtained as $\boldsymbol{\theta} = \boldsymbol{\theta}^{(2L+1)}$. Note that only the $M \times M$ matrices \mathbf{D}_k have to be inverted.

6. SIMULATION RESULTS

TFAR Process. We defined a TFAR process of length $N = 256$ and order $(M, L) = (4, 2)$ with specified coefficients $a_{m,l}$ and σ_l . We generated a *single* realization $x[n]$ via (3) and estimated the EAF from this realization according to (13) with $I = 1$, using $\Psi[m, l] = w_1[m] w_2[l]$ with $w_1[m]$ and $w_2[n]$ (the Fourier transform of $w_2[l]$) chosen as Hanning windows of length 49. We then calculated estimates of $a_m[n]$ and $\sigma[n]$ by solving the exact and approximate TF Yule–Walker equations using the true model order $(M, L) = (4, 2)$ and subsequently inserting the resulting estimates $\hat{a}_{m,l}$, $\hat{\sigma}_l$ into (4), (5). For comparison, we also estimated $a_m[n]$ and $\sigma[n]$ using Grenier’s method [5]. By way of example, Fig. 2 shows the true parameter function $a_1[n]$ and the corresponding estimates. It is seen that all three methods yield reasonable estimation results.

For a better assessment of performance, we repeated this experiment 100 times to obtain estimates of the overall normalized mean-square parameter estimation error ε . The performance was best for the exact TF Yule–Walker equations ($\varepsilon = 0.107$), second best for the approximate TF Yule–Walker equations ($\varepsilon = 0.119$), and poorest for Grenier’s method ($\varepsilon = 0.136$, i.e., about 30% larger than for the exact TF Yule–Walker equations). In fact, the estimation variance exhibited by Grenier’s method was observed to be significantly larger than that of our methods.

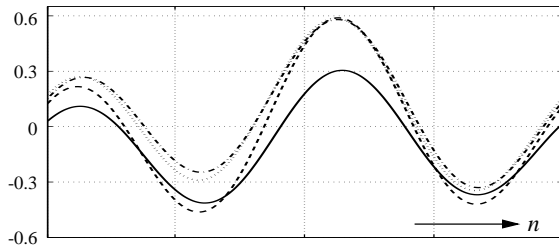


Figure 2: True parameter function $a_1[n]$ (solid line) and estimates obtained from the exact TF Yule-Walker equations (dashed line), the approximate TF Yule-Walker equations (dotted line), and Grenier's method (dash-dotted line).

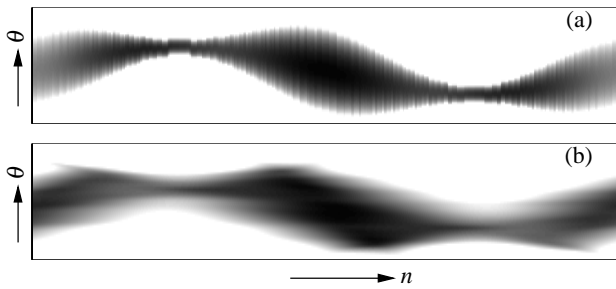


Figure 3: Comparison of (a) the specified (non-TFAR) time-varying spectrum and (b) the TFAR spectrum estimated from a single realization $x[n]$.

Non-TFAR Process. Next, we used the method described in [17] to synthesize a single realization $x[n]$ of a *non-TFAR* process of length $N = 4096$ from the specified time-varying spectrum shown in Fig. 3(a). The EAF was estimated from this realization according to (13), using $\Psi[m, l] = w_1[m] w_2[l]$ with $w_1[m]$ and $w_2[n]$ chosen as Hanning windows of length 41 and 81, respectively. We then calculated sets of TFAR parameters $a_m[n]$ by solving the approximate TF Yule-Walker equations for model orders $M \in [21, 27]$ and $L \in [1, 3]$. As final estimates $\hat{a}_m[n]$ and $\hat{\sigma}[n]$, we retained the results obtained for the M and L for which the energy of $e[n]/\hat{\sigma}[n]$ was minimum. (The error signal $e[n]$ was calculated by means of the inverse filter (15).) A time-varying spectrum estimate was then determined as

$$\hat{S}(n, \theta) = \frac{\hat{\sigma}^2[n]}{\left| \sum_{m=1}^{\hat{M}} \hat{a}_m[n] e^{-j2\pi\theta m} \right|^2}$$

(see Fig. 3(b)). The normalized energy of the difference between the specified spectrum in Fig. 3(a) and the estimated spectrum in Fig. 3(b) was 17%.

We then repeated the above experiment for 50 different realizations. In all cases, the estimated spectral model order was $\hat{L} = 2$. A histogram of the estimated temporal model order \hat{M} is shown in Fig. 4(a). Furthermore, Fig. 4(b) shows a histogram of the normalized energy of the difference between the specified spectrum and the estimated spectra obtained from the individual realizations.

7. CONCLUSIONS

We presented a new formulation of nonstationary autoregressive (AR) modeling in terms of time-frequency (TF) shifts. The proposed *TFAR model* is physically intuitive and highly parsimonious. Its parameters are determined by *TF Yule-Walker equations* that can be solved efficiently due to their block-Toeplitz structure. For moderate model orders, an approximate version of the TF Yule-Walker equations allows the use of an even faster algorithm. Numerical simulations demonstrated the good performance of the proposed techniques for nonstationary modeling and spectrum estimation. Our

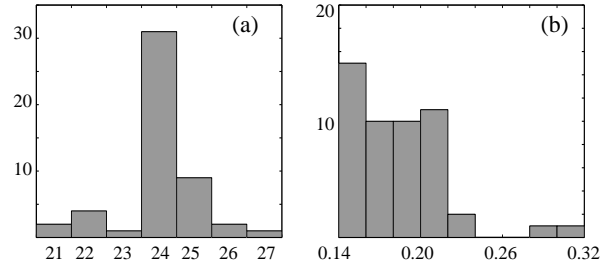


Figure 4: (a) Histogram of the estimated temporal model order \hat{M} ; (b) histogram of the normalized difference energy between the prescribed spectrum and the estimated spectra.

future work will address the estimation of the TFAR model orders M, L and the definition and estimation of TFARMA models.

REFERENCES

- [1] S. M. Kay, *Modern Spectral Estimation*. Englewood Cliffs (NJ): Prentice Hall, 1988.
- [2] P. Stoica and R. Moses, *Introduction to Spectral Analysis*. Englewood Cliffs (NJ): Prentice Hall, 1997.
- [3] T. S. Rao, "The fitting of non-stationary time-series models with time-dependent parameters," *J. Roy. Stat. Soc. Ser. B*, vol. 32, no. 2, pp. 312–322, 1970.
- [4] L. A. Loporace, "Linear estimation of nonstationary signals," *J. Acoust. Soc. Amer.*, vol. 58, pp. 1288–1295, Dec. 1975.
- [5] Y. Grenier, "Time-dependent ARMA modeling of nonstationary signals," *IEEE Trans. Acoust., Speech, Signal Processing*, vol. 31, pp. 899–911, Aug. 1983.
- [6] G. Alengrin, M. Barlaud, and J. Menez, "Unbiased parameter estimation of nonstationary signals in noise," *IEEE Trans. Acoust., Speech, Signal Processing*, vol. 34, pp. 1319–1322, Oct. 1986.
- [7] J. P. Kaipio and M. Juntunen, "Deterministic regression smoothness priors TVAR modelling," in *Proc. IEEE ICASSP-99*, (Phoenix, AZ), pp. 1693–1696, May 1999.
- [8] R. Ben Mrad, S. D. Fassois, and J. A. Levitt, "A polynomial-algebraic method for non-stationary TARMA signal analysis—Part I: The method," *Signal Processing*, vol. 65, pp. 1–19, Jan. 1998.
- [9] A. T. Moser and D. Graupe, "Identification of nonstationary models with application to myoelectric signals for controlling electrical stimulation of paraplegics," *IEEE Trans. Acoust., Speech, Signal Processing*, vol. 37, pp. 713–719, May 1989.
- [10] W. Kozek, F. Hlawatsch, H. Kirchauer, and U. Trautwein, "Correlative time-frequency analysis and classification of nonstationary random processes," in *Proc. IEEE-SP Int. Sympos. Time-Frequency Time-Scale Analysis*, (Philadelphia, PA), pp. 417–420, Oct. 1994.
- [11] G. Matz and F. Hlawatsch, "Time-varying power spectra of nonstationary random processes," in *Time-Frequency Signal Analysis and Processing* (B. Boashash, ed.), Englewood Cliffs (NJ): Prentice Hall, 2002.
- [12] W. Martin and P. Flandrin, "Wigner-Ville spectral analysis of nonstationary processes," *IEEE Trans. Acoust., Speech, Signal Processing*, vol. 33, pp. 1461–1470, Dec. 1985.
- [13] E. Feig, "Estimating interesting portions of the ambiguity function," in *Signal Processing, Part I: Signal Processing Theory* (L. Auslander, T. Kailath, and S. Mitter, eds.), pp. 70–73, New York: Springer, 1990.
- [14] J. Makhlouf, "Linear prediction: A tutorial review," *Proc. IEEE*, vol. 63, pp. 561–580, April 1975.
- [15] H. Akaike, "Block Toeplitz matrix inversion," *SIAM J. Appl. Math.*, vol. 24, pp. 234–241, March 1973.
- [16] M. Wax and T. Kailath, "Efficient inversion of Toeplitz-block Toeplitz matrix," *IEEE Trans. Acoust., Speech, Signal Processing*, vol. 31, pp. 1218–1221, Oct. 1983.
- [17] G. Matz and F. Hlawatsch, "Linear time-frequency filters: Online algorithms and applications," in *Applications in Time-Frequency Signal Processing* (A. Papandreou-Suppappola, ed.), Boca Raton (FL): CRC Press, 2002.